Study of Scattering Distribution for Spherical Particles

Diksha Garg[1], Aparajita Bandyopadhyay[2], Amartya Sengupta[1]

[1]*Department of Physics, Indian Institute of Technology Delhi, New Delhi, India.*

[2]*Joint Advanced Technology Center, Indian Institute of Technology Delhi, New Delhi, India.*

Corresponding Author: amartya@physics.iitd.ac.in

Abstract:

In the present study, scattering contribution of spherical particles in frequency range from 0.5 THz to 2.6 THz is examined using COMSOL Multiphysics®. For simulation, three materials of different optical properties are considered, namely, sugar, sugar-free powder and *Teflon*. For precise analysis, refractive indices of the samples were obtained using Terahertz time domain spectroscopy (THz-TDS) and varied with frequency. With particle sizes of 20 µm and 100 µm, variation of scattering losses and electric field distribution of scattered radiation is evaluated for each material. Transformation of the scattering response from symmetric distribution to asymmetric distribution is observed with increase in frequency which can be related to the transition from Rayleigh to Mie scattering.

Keyword: Terahertz spectroscopy, scattering, optical constants of material

Introduction:

The terahertz (THz) region of the electromagnetic (EM) spectrum is located in between the mid-infrared and microwave region. It bridges the gap between the classical to the quantum region of the EM spectrum and corresponds to the frequency range from 0.1 THz to 10 THz (or wavelength from 3000 µm to 30 µm) [1]. THz spectroscopy has several advantages over other spectroscopy, therefore, it has found widespread applications in various fields. Unlike X-rays, these radiations are non-ionizing due to their low photon energy (4.1 meV at 1 THz). The non-ionizing property of THz makes it suitable for biological, pharmaceutical, food and other samples. High sensitivity to the presence of water is one of the unique properties of THz waves which provides a way of water content estimation in plant samples for proper irrigation management in agriculture sector [2]. Also, THz waves can penetrate most non-polar dielectrics, which means that THz can see through visually opaque materials such as packaging and clothing [3]. For most materials, the vibrational and rotational energies of the molecule lie in the THz region which is further used in many applications such as chemical sensing [4], material characterization [5], and security screening [6]. The unknown samples can be identified based on their spectral signature. However, there are some obstacles which can influence the true spectral signature of the material and make the identification difficult. One of the barriers is the Mie scattering responsible for the distortion and alteration of the absorption peaks. Hence, to obtain the accurate spectral features of any material, elimination of scattering effects from experimentally acquired result is necessary.

Scattering depends on the randomness: asymmetric shape, size and morphology of the sample, and becomes predominant if the examined sample is in granular form. Scattering plays an important role in the THz region as most of the granular samples, especially food and bio samples, have grain sizes comparable to the THz wavelength. The angular distribution of scattered radiation is not always symmetric and depends on the relative size of the scattering particle. In case of smaller particles, which scatter isotropically, simple theory of Rayleigh scattering can be applied. However, for larger particles, Mie scattering occurs which is more pronounced in the forward direction and cannot be estimated easily. Some previous work has been reported to minimize the scattering effect for granular samples [7-9]. Yet, methodologies to remove the scattering effect for a material having complex structure is quite challenging.

Prior knowledge of scattering effect is essential for effective experimental data analyses. COMSOL Multiphysics® is an ideal modeling software to realize the complex problems such as scattering. It is a fast, reliable, and cost-effective simulation tool which provides a user-friendly environment to deal with innovative ideas in real world applications. Single design can be used to perform a comparative study of various materials.

The current work is motivated by an experimental THz spectroscopic measurement for two granular samples: sugar and sugar-free [10]. Garg et al. shows the frequency spectra influenced by scattering due to the granular nature of the samples. In the current study, scattering losses for spherical particle of different size is calculated. Also, the corresponding change in the distribution of electric field is estimated. Sugar and sugar-free powder, the samples under consideration, have sucrose and lactose as their main constituents respectively. *Teflon* which is transparent in the given frequency range is used as a reference for comparison. Material properties such as the real and imaginary part of the refractive index used in the simulation were acquired using THz-time domain spectroscopy (THz-TDS).

Theory:

If a polarized light is incident on any medium, dipole charges generate in the medium due to the interaction of incident electric field with medium particles. These generated dipole charges redistribute the electric field falling on the medium. Loss due to redistribution or extinction depends on size, composition, refractive index, orientation of the particles, and wavelength of the incident radiation.

If the radius of the particle is very small compared to the wavelength of the incident radiation, Rayleigh scattering occurs; whereas, Mie scattering arises in case of larger particles. In Rayleigh scattering, the intensity of the scattered radiation varies with the fourth power of frequency. As the particle size increases, this relation between scattered field and frequency vanishes due to strong particle-radiation interaction. Mie theory, based on the solution of Maxwell's equations [11], provides a rigorous analytical expression for scattering by a homogeneous medium containing a spherical particle of arbitrary size.

Scattering cross-section is a parameter used to define the scattering responses and can be described as the ratio of rate of energy flow of scattered radiation to the intensity of incident radiation [12].

$$C_{sca} = \frac{W_{sca}}{I_i}$$

Here, W_{sca} is the net rate of energy flow crossing the surface of the particle, defined as the integral of the time averaged Poynting's vector of scattered field across the particle surface.

$$W_{sca} = \oint S.dA$$

And, I_i is the intensity of incident radiation which is given as,

$$I_i = < S_i > = \frac{1}{2Z_0} {E_o}^2$$

Z_0 is the impedance of free space, E_o is the electric field amplitude of incident radiation.

Proposed simulation model:

The proposed 3D model is simulated using Electromagnetic Waves-Frequency Domain interface available in wave optics module. Spherical particles of different radii: 20 μm and 100 μm were simulated for sugar and sugar free powder. In each case, the perfectly matched layer (PML) was selected with radius ten times the radius of the particle and with thickness three times the particle radius. Air (refractive index =1) is used in the surrounding environment of the spherical particle. The incident waves were assumed to be propagating in the positive z-direction with linear polarization along x-axis. Material considered for the particles were user-defined to have variable refractive indices with frequency. The real part of refractive index is related to the material dispersion response while the imaginary part defines the material absorption. Plot for imaginary part of the refractive index of each sample is shown in figure 1. There is no absorption peak for *Teflon* while, both sugar and sugar-free has absorption peaks in the considered frequency range.

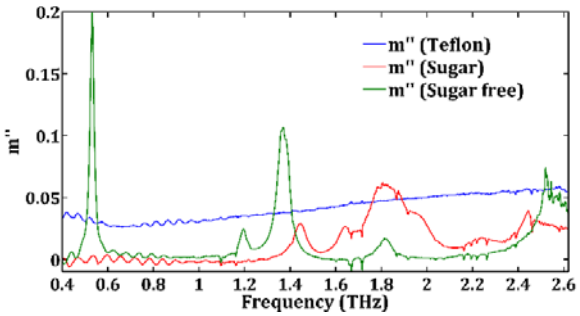

Figure 1. Plot for imaginary part of refractive index for sugar, sugar free powder, and *Teflon*.

PML layer and particle domain were discretized using physics-controlled mesh elements. Scattering cross-section were calculated using parametric sweep in the defined frequency range with step size 1GHz.

Results and discussion:

In figure 2, scattered electric field for *Teflon* particle with radius 20 µm and 100 µm at three different frequencies 0.5 THz, 1.16 THz and 2.6 THz is shown.

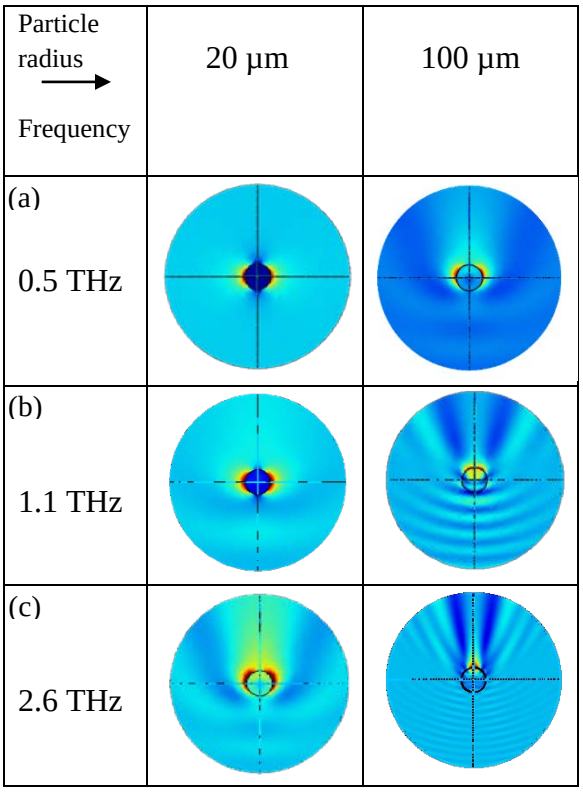

Figure 2. Scattered electric field for *teflon* of 20 µm and 100 µm radius at frequencies; a) 0.5 THz, b) 1.5 THz, and c) 2.6 THz.

Obtained plots are in the z-x plane, incident waves are propagating in the upward direction while the polarization is in horizontal direction. In case of 20 µm radius, the electric field retains its polarization state at low frequencies due to the less interaction between particle and incoming radiation. The wavelength of incident radiation is very large outside (~ 600 µm) as well as inside the particle (refractive index is shown in fig 1), hence, scattering distribution follows Rayleigh scattering. As the frequency of incident radiation increases (or corresponding wavelength decreases), electric field is directed towards the forward direction i.e. in the positive z-direction. It is observed that electric field penetrates through the particle for larger frequencies due to the strong scattering interaction.

For 100 µm radius, due to the large particle size, electric field is primarily in the forward direction even at smaller frequency (0.5 THz). For higher frequencies, when particle size is comparable to the wavelength of incident radiation, alternative minima and maxima were observed due to the diffraction. This distribution can be estimated by the theory of geometrical optics.

Scattering cross-section of each sample with 20 µm radius is shown in Figure 3. As expected, scattering cross-section (C_{sca}) is small for initial frequency values and increases with the frequency. It is observed that the change in the C_{sca} is comparatively large in case of *teflon*.

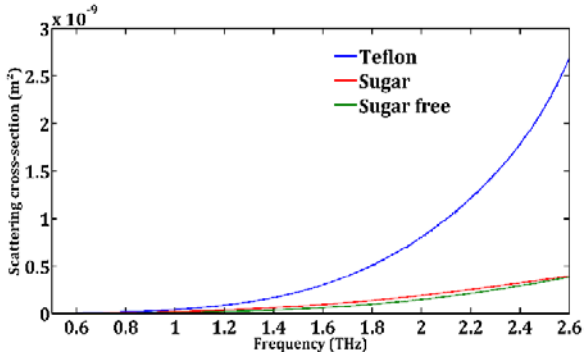

Figure 3. Plot for scattering cross-section of each particle with radius 20 µm.

Variation in C_{sca} for different materials can be understood based on their complex refractive index. There is no absorption for *teflon* (fig 1) in the described frequency range while sugar and sugar free powder have significant absorption edges. Presence of absorption prevents the radiation and does not allow it to penetrate through the particle. Therefore, it leads to

a decrease in the total scattering cross-section in comparison to a non-absorbing *teflon*.

Scattering cross-section for 100 µm particle size is shown in figure 4. Due to the large particle size, scattering for each particle increases significantly as compared to previous case. For non-absorbing *Teflon*, series of board minima and maxima were obtained due to the interference of incident and forward-scattering radiation. Maxima corresponds to the constructive interference, whereas minima relates to the condition of destructive interference. In case of sugar and sugar free powder, scattering is less in comparison to *teflon* because of the absorbing nature of these materials. As discussed above, radiation is absorbed in the particle; consequently, less radiation can pass through the particle. Although, scattering is less for sugar and sugar free powder, but it increases conventionally with frequency.

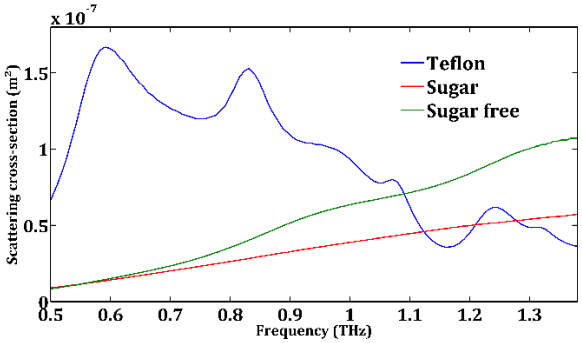

Figure 4. Plot for scattering cross-section of each particle with radius 100 µm.

Conclusions and future scope:

COMSOL provides a good understanding of different optical responses for a wide range of frequency. Based on the COMSOL results, a frequency range can be defined for the precise study of different optical phenomenon. The simulated model can help to eliminate the scattering effect from the frequency spectra, and it can be extended to predict the scattering contribution from complex material for real time applications. In the study, it was observed that scattering response differs for absorbing and non-absorbing particles and increases with particle size. In future, we plan to study scattering response for large number of particles of different sizes. Results will be further utilized to get the accurate spectral signature of materials using THz-TDS.

Acknowledgements:

1. Defence Research and Development Organization (DRDO) vide Grant #DFTM/03/3203/M/JATC.
2. Department of Atomic Energy- Board of Research in Nuclear Sciences (DAE-BRNS) vide Grant # 37 (3)/14/01/2016-BRNS/37015.
3. University Grants Commission, Ministry of Human Resource Development (UGC-MHRD) vide Award # 1349/CSIR-UGC NET/Dec2017.

References:

1. Lewis, Terahertz physics, pp. 205-230, Cambridge University Press, (2012).
2. Gente et al., 'Determination of leaf water content from terahertz time-domain spectroscopic data' J Infrared Milli Terahz Waves, 34, 316–323, (2013).
3. Zhang and Xu, Introduction to THz wave photonics, pp. 1-9, Springer, New York (2010).
4. Fischer et al. 'Chemical recognition in terahertz time-domain spectroscopy and imaging', Semicond. Sci. Technol., 20, S246–S253 (2005).
5. Naftaly and Miles, 'Terahertz time-domain spectroscopy for material characterization', Proceedings of the IEEE, 95, No. 8, (2007).
6. Xin et al. 'Terahertz imaging system for remote sensing and security applications', 3rd Asia Pacific conference on Antenna and Propagation, pp. 1335-1338 (2014).
7. Shen et al. 'Elimination of scattering effects in spectral measurement of granulated materials using terahertz pulsed spectroscopy', Appl. Phys. Lett., 92, 051103 (2008).
8. Zurk et al., 'Terahertz scattering from granular material' JOSA B 24, 9 (2007).
9. Bandyopadhyay et al., "Effects of scattering on THz spectra of Granular solids" Int J Infrared Milli Waves, 28,969–97 (2007).
10. Garg et al., 'Scattering: Challenge of Terahertz Time Domain Spectroscopy' Frontiers in Optics / Laser Science, OSA conference (2019).
11. H.C. van de Hulst, Light scattering by small particles, Chap. 9, Dover publications, (1981).
12. Bohren and Huffman, Absorption and scattering of light by small particles, Chap. 4, Wiley publication, (1983).